

Dynamics of the Pavo-Indus and Grus clouds of galaxies^{*}

P. Fouqué^{1,2}, D. Proust¹, H. Quintana² and A. Ramirez²

¹ Observatoire de Paris-Meudon F-92195 Meudon Cedex, France

² Pontificia Universidad Católica, Grupo de Astrofísica, Casilla 104, Santiago, Chile

Received September 30; accepted February 16, 1993

Abstract. — A study of groups of galaxies in the above regions was carried out by selecting a sample extending one magnitude deeper than previous work in the area, complete down to 15 mag. We report new redshift determinations for 58 galaxies in the region and 13 other miscellaneous galaxies, based on La Silla observations. Using a total of 266 galaxies with measured redshifts in the Pavo-Indus and Grus clouds, we perform a new analysis of groupings following a well-tested algorithm. A total of 18 groups is singled out, most of them known from previous work, even though a few additional members are added. For all the groups, we have calculated dynamical parameters and M/L ratios. All groups are found to be bound aggregates, but only one group can be virialized. For the 6 most populated examples, having at least 5 members, we also calculate several mass estimators and discuss the wide range of observed M/L ratios, which extends from 9 to nearly $500 M_{\odot}/L_{\odot}$. We introduce two parameters to measure the presence of either a dominant galaxy or internal subcondensations, respectively, and test whether any correlation with the M/L ratios can be detected. No clear correlations are found, though some weak tendencies appear, which need a wider database to be tested.

Key words: galaxies: clustering — galaxies: distances and redshifts

1. Introduction

One of the outstanding problems in astrophysics concerns the missing mass of the Universe: 90 % of the mass of the Universe appears to be invisible. Several arguments show that luminous mass cannot give account of dynamical effects. One of these is the high mass-to-luminosity ratio usually found in groups and clusters of galaxies.

These ratios are computed assuming that groups of galaxies are virialized entities. The actual mass of not yet virialized bound aggregates of galaxies is probably of the same order of magnitude as the mass calculated assuming that the group is virialized, but the precise ratio is unpredictable. Evidence that groups of galaxies, and at least some clusters, have not yet reached a virialized status, is growing. The time to reach virialization is larger than the age of the Universe, for many observed systems. Moreover, many clusters of galaxies show subcondensations (Dressler & Shectman 1988), which might be accreted small groups not yet well mixed with the remaining galaxies of the cluster. These results force us to look more closely for truly virialized aggregates, in order to see whether these contain missing mass or not.

In order to search for such entities, we recently compiled a catalogue of groups of galaxies within 80 Mpc ($H_0 = 75 \text{ km s}^{-1} \text{ Mpc}^{-1}$) (Fouqué et al. 1992) using a revised hierarchical algorithm (Materne 1978; Tully 1987), described in Gourgoulhon et al. (1992). One shortcoming of our algorithm is that, in order to correctly take account of incompleteness at increasing distances, it must use a complete sample, down to some limiting magnitude or diameter. Our whole sky catalogue used a sample limited to a diameter of 100 arcsec, roughly corresponding to a limiting magnitude of 14. A group is recognized as such only if it contains at least three members. Therefore, groups at moderate distances were missed due to the limited depth of the whole sample.

2. The sample

We decided to investigate selected regions by using deeper samples. The present work deals with one of such regions, where de Vaucouleurs (1975) identified two clouds of galaxies, namely Pavo-Indus and Grus (his groups G45 and G27, respectively). These clouds belong to the connection between the Indus Supercluster and our Local Supercluster. The coordinates limits of our surveyed regions are: $21^{\text{h}}25$ to $22^{\text{h}}39$ (α_{2000}) and -40° to -51.66°

^{*} Observations collected at the European Southern Observatory, La Silla, Chile

(δ_{2000}) for Pavo-Indus, and 22^h5 to 23^h71 (α_{2000}) and -45° to -30° (δ_{2000}) for Grus.

Within these limits, we selected from the PGC catalogue of galaxies (Paturel et al. 1989a, 1989b) all objects with a listed magnitude brighter than 15. These *B*-band magnitudes, which come from various sources (see PGC for details), mainly from ESOLV (Lauberts & Valentijn 1989), are homogenized to the RC3 system (de Vaucouleurs et al. 1991). After correction for extinction effects, the limiting magnitude becomes 14.5. We found 121 objects in the Pavo-Indus region, and 117 in the Grus region. However, looking at the ESO and SERC sky survey films, we noted the following corrections to the PGC catalogue:

PGC 66429 = ESO 235-G?81 could not be found on the films at its ESO coordinates.

PGC 66924 = ESO 236-IG19 consists of two galaxies, noted ESO 236-19N (= 236 0190 in ESOLV) and ESO 236-19S (= 236 0191 in ESOLV).

PGC 67385 is clearly fainter than 15 mag. Its magnitude in PGC is an estimate derived from its diameter (Paturel et al. 1987).

PGC 68283 = ESO 288-G51 and PGC 68284 = ESO 237-G46 = IC 5170 are one and the same galaxy (see ESOLV and Paturel et al. 1991).

PGC 69046 = NGC 7297 has a companion, which is not in the PGC catalogue, but appears to be bright enough to deserve inclusion into our sample as NGC 7297 cmp.

PGC 69273 = ESO 468-G16 is not MCG -5-53-18, but MCG -5-53-20. MCG -5-53-18 is the fainter galaxy at $5'$ W and $1.5'$ N. It is not in the PGC catalogue, but appears to be bright enough to deserve inclusion into our sample.

PGC 70311 = MCG -7-47-12 could not be found on the films at its (imprecise) MCG coordinates.

PGC 70787 is a strange object at $2.9'$ E from NGC 7531. It is not a plate default, as it appears on red and blue ESO films, as well as on SERC films.

PGC 70857 could not be found on the films at its (imprecise) coordinates (Karachentseva 1973). Perhaps NGC 7552.

Moreover, we added to the sample a few galaxies fainter than our limit, but with a known recession velocity. The total samples for Pavo-Indus and Grus regions are 142 and 136, respectively. Among these, 208 had known recession velocities at the time we began this program. Our goal was then to measure the redshift of the other galaxies, and we succeeded for 58 of them. Only 12 over 278 remain to be measured to reach the completeness limit $B_T = 15$, if we admit that the PGC catalogue is complete down to this limit. Figure 1 shows a histogram of magnitudes for 246 galaxies of the sample with a true measure of magnitude (i.e. not derived from diameter) and

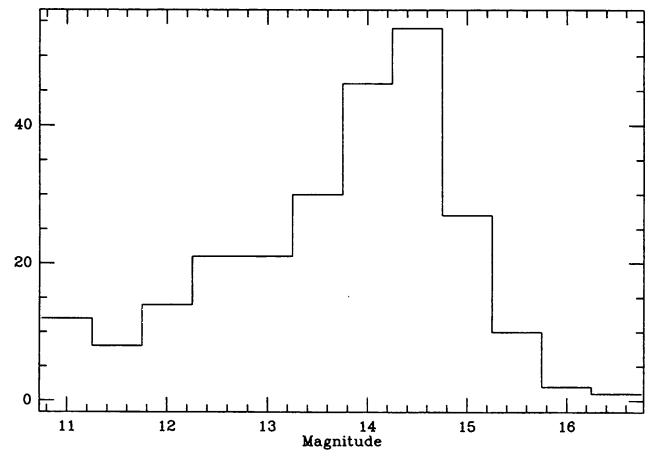


Fig. 1. Histogram of corrected *B*-magnitudes for 246 galaxies

a redshift. It confirms our adopted limit of completeness, at $B_T^0 = 14.5$.

3. Observations

The spectroscopic observations were conducted at La Silla (Chile) in September 1990 at the 1.52 m telescope, equipped with the Boller and Chivens spectrograph at its Cassegrain focus. A 600 lines/mm grating, blazed at 4500 \AA in the first order, was used. The dispersion was 127 \AA/mm . The detector was an excellent 1024×1024 Thomson 1K coated CCD, with a pixel size of $19 \text{ }\mu\text{m}$. The slit width was set at 2 arcsec, giving a projected slit-width of 2 pixels, and a resolution of 4.7 \AA . The spectral coverage was 4250 \AA to 6710 \AA . A binning of two pixels perpendicular to the dispersion was used.

Before each science exposure, a calibration with a He-Ar lamp was made. Then a first exposure of 30 min was acquired. If the spectrum appeared under-exposed, a second calibration and a second exposure, generally of 30 min, were performed. Several bias and dome flat-fields frames were exposed each afternoon, and averaged before the night, thus allowing a quick on-line reduction. No dark frame was found necessary, because the read-out noise was typically 5 e^- , while the dark current amounted to 0.5 e^- for 30 min exposures.

The same template star for cross-correlation was observed each night, namely HD 176047 (spectral type K1 III). When the seeing was good, it was moved across the slit during its 30 sec exposure, in order to cover all the pixels in the slit. Its heliocentric radial velocity is given by Maurice et al. (1984) as $-42.8 \pm 0.1 \text{ km s}^{-1}$. Well-exposed

Table 1. New velocities of 58 galaxies in the Pavo-Indus and Grus regions

PGC	Name	α_{1950}	δ_{1950}	V_{\odot}	σ	Note	B_T°
66430	ESO286-80	21 12 12.0	-46 59 18	11353	58		14.23
66436	ESO286-82	21 12 31.0	-42 38 06	4950	48		14.17
66502	ESO287-02	21 14 14.0	-42 33 00	5412	44		14.44
66701	ESO287-18	21 21 23.0	-42 48 24	5027	45		14.24
66720	ESO342-42	21 22 12.0	-40 20 18	5833	43		14.16
66740	IC5105B	21 22 51.0	-41 03 06	2270	em		13.06
66760	ESO287-26	21 23 08.0	-43 26 18	5293	49		14.38
66785	NGC7061	21 24 05.0	-49 16 54	9063	49		14.01
66839	ESO342-52	21 25 55.0	-41 59 48	9328	40		13.96
66870	NGC7072A	21 27 13.0	-43 25 18	5069	83		14.94
66873	ESO287-30	21 27 21.0	-44 39 00	10911	68		14.39
66892	ESO287-32	21 28 12.0	-43 28 42	5436	86	*	14.65
66919	ESO236-18	21 28 55.0	-48 13 30	7060	40		14.36
66924	ESO236-19N	21 28 59.0	-48 25 36	9285	75		14.54
66924	ESO236-19S	21 28 57.0	-48 26 00	9261	81		15.16
66979	ESO343-07	21 31 11.0	-41 03 00	5119	38		14.40
67048	ESO287-39	21 33 21.0	-45 17 24	2718	96	*	14.39
67061	ESO287-40	21 34 12.0	-47 15 36	9308	49		14.07
67073	ESO287-41	21 34 57.0	-42 59 12	2499	89		14.51
67080	ESO236-26	21 34 56.0	-47 59 54	5272	98		14.67
67128	ESO287-45	21 36 45.0	-43 06 24	4814	40		14.14
67184	SGC	21 38 32.7	-47 03 00	9481	53		
67238	ESO343-24	21 40 21.0	-40 21 12	4692	68		13.87
67716	SGC	21 54 26.6	-45 39 13	18292	52		
67772	SGC	21 55 48.0	-48 03 20	17398	40		
67852	ESO288-30	21 58 28.0	-42 41 42	7959	60		14.30
67854	ESO288-32	21 58 33.0	-42 40 48	8080	em		14.60
68183	ESO237-42	22 06 35.0	-50 02 42	8102	66		14.24
68215	ESO288-45	22 07 35.0	-43 30 00	2236	71		14.19
68314	ESO237-47	22 10 04.0	-49 05 36	10717	43		14.47
68366	ESO344-15	22 11 32.0	-40 54 54	17061	49		
68403	ESO289-05	22 12 02.0	-46 31 54	1960	em		14.39
69046	NGC7297	22 28 16.0	-38 05 00	10990	42		14.14
	NGC7297cmp	22 28 14.0	-38 05 12	10735	52		
69060	NGC7299	22 28 39.0	-38 04 00	9091	43		14.71
69103	ESO345-21	22 29 44.0	-38 18 24	3141	49		14.23
69133	ESO289-37	22 30 21.0	-44 48 30	1221	71		14.54
69168	ESO405-29	22 31 13.0	-32 39 18	3629	62		14.45
69178	ESO345-28	22 31 22.0	-38 25 18	9120	42		14.59
69234	ESO345-32	22 32 33.0	-37 39 24	11383	41		14.74
69238	ESO405-31	22 32 38.0	-35 22 54	8631	46		14.04
69239	ESO289-42	22 32 32.0	-44 40 06	1720	em		14.38
69244	ESO345-33	22 32 42.0	-37 37 30	11673	52		14.63
69273	ESO468-16	22 33 21.0	-31 59 12	8024	55		14.55
	MCG-5-53-18	22 32 56.0	-31 57 54	8055		*	
69440	ESO289-47	22 36 55.0	-44 07 18	10123	53		13.96
69567	ESO345-44	22 40 01.0	-42 18 30	9394	55		14.71
69593	ESO290-07	22 40 39.0	-44 09 36	9568	63		14.08
	ESO406-10	22 42 04.0	-34 28 33	8731	87	*	14.52
69669	ESO406-11	22 42 57.0	-35 28 12	8685	33		14.23
	ESO406-18N	22 51 27.0	-37 21 00	17240	em		14.39
70030	ESO406-21	22 53 05.0	-34 27 36	8702	36		14.55
70109	ESO406-31	22 54 54.0	-35 39 54	1553	67		14.15
70293	ESO346-24	22 59 07.0	-40 55 30	10023	55		14.41
70407	ESO407-02	23 01 56.0	-34 19 36	1708	32		13.91
70645	IC5289	23 08 36.0	-32 45 00	11213	57		13.98
71385	SGC	23 22 28.5	-44 27 13	10489	24		
71660	ESO347-20	23 28 50.0	-42 25 24	1840	em		14.59

Notes :

ESO287-32 : emission lines ($H\alpha$, $H\beta$) give $V = 5160 \text{ km s}^{-1}$.ESO287-39 : emission lines ($H\alpha$, $H\beta$, $O II$) give $V = 2260 \text{ km s}^{-1}$.

MCG-5-53-18 : uncertain velocity.

ESO406-10 : double galaxy, slit between both.

galaxies of our program were also used as templates to verify the results from this star.

The spectra reduction was carried out using the IHAP image processing software at ESO-Garching, and the recession velocities were derived from a cross-correlation procedure developed at Paris Observatory, within the frame of the EVE image analysis package. Wavelength calibration was performed using the He-Ar lamp reference. The lines positions are fitted with a third order polynomial; the average rms of the calibration is 0.18 pixel, and the resolution, as measured from the FWHM of a Gaussian fit to the He-Ar lines, is 5 Å.

Table 2. New velocities of 13 other galaxies

PGC	Name	α_{1950}	δ_{1950}	V_{\odot}	σ	Note
11791	ESO031-11	03 09 37.0	-74 11 48	8350	87	*
11933	ESO481-10	03 10 08.0	-26 24 30	6451	98	
11934	ESO481-09	03 10 07.0	-24 48 30	12253	50	
13027	IC1947	03 29 03.0	-50 30 24	11545	59	*
15784	ESO251-19	04 38 46.0	-43 24 48	2377	94	*
61835	IC4709	18 20 05.0	-56 23 48	5068	80	
62246	IC4739	18 36 14.0	-61 56 54	4530	em	*
62495	IC4782	18 46 45.0	-55 33 00	2870	em	
62492	ESO183-17	18 46 41.0	-55 34 00	2750	em	
63743	ESO283-20	19 47 54.0	-44 58 18	5751	45	
65426	IC5026	20 41 55.0	-78 15 12	2750	em	*
66357	ESO342-22	21 09 47.0	-38 04 36	12858	41	
66361	ESO342-23	21 09 54.0	-38 05 36	13140	em	

Notes:

ESO031-11: we measured the elongated object (labelled 31 0110 in ESOLV); Fairall (1980) gives $V = -1290$ for a western companion (Fairall 232, which is not ESO031-11, as stated in PGC). The south-eastern companion (PGC 11795) is labelled 31 0111 in ESOLV.

IC1947: Chincarini et al. (1984) give $V = 42$.

ESO251-19: da Costa et al. (1991) give $V = 50 \pm 28$, but note that the spectrum is probably contaminated by a star.

IC4739: star superimposed; RC3 (de Vaucouleurs et al. 1991) gives $V = -38$, from Huchra (ZCAT August 1988, Las Campanas measurement).

IC5026: our measurement is uncertain (H α , O II); da Costa et al. (1991) give $V = 15 \pm 32$, but note that the spectrum is contaminated by a star.

The spectra were rebinned with a scale of 1 Å/bin equally spaced in log wavelength and the velocity was derived from the cross-correlation procedure with stellar spectra of known radial velocity obtained the same night, according to Tonry & Davis (1979). In order to test the accuracy of the radial velocities derived from the cross-correlation procedure, we have fitted a gaussian profile to the correlation peak; the accuracy of the redshift determination is obtained from the width at half-height of the peak. Table 1 lists new heliocentric velocities for 58

galaxies in this region and their accuracy (*em* means that only emission lines could be measured), and Fig. 2 shows a histogram of the velocities for the 266 galaxies measured.

Due to the mounting of the telescope, observations at low declinations are limited to one side of the meridian. Resulting free time was used to measure some galaxies with discrepant redshifts in the literature, or interesting objects from other programmes. Part of these measures have been published elsewhere (Bottinelli et al. 1992, under label ESO 5; Proust et al. 1992, Abell 151 #53 and #65). The remaining 13 galaxy velocities are given in Table 2.

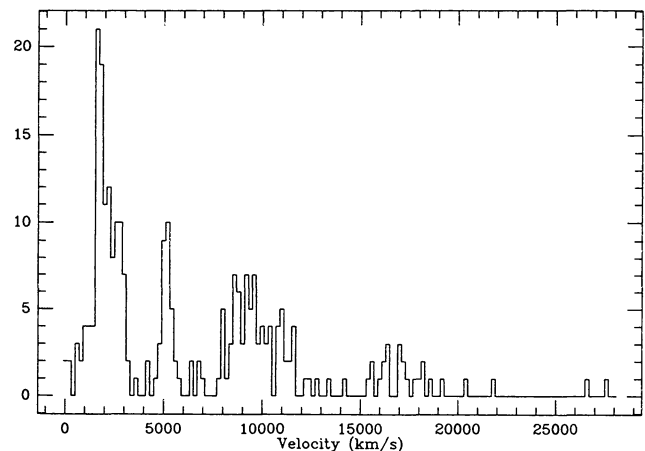


Fig. 2. Histogram of heliocentric velocities of the 266 measured galaxies. Holes around 3500 and 7500 km s⁻¹ are noticeable

4. The results

Although our sample is deeper by about 1 mag. than the all-sky sample used in Fouqué et al. (1992), only 8 among 58 newly measured galaxies are found to belong to the Pavo-Indus-Grus groups. The remaining belong to the background. The limiting recession velocity, up to which our results are credible, was given in Gourgoulhon et al. (1992) as $V_{\text{lim}} = 8.6 \cdot 10^{0.2m_{\text{lim}}}$. This corresponds to $V_{\text{lim}} = 8600 \text{ km s}^{-1}$ for our limiting magnitude 15. However, this limit corresponds to a galaxy with the L^* luminosity (knee of the Schechter luminosity function). A group at that distance needs three such galaxies to be detected. As there is no galaxy in our sample with recession velocities between 7060 and 7849 km s⁻¹ (see Fig. 2), we prefer setting the limit at 7500 km s⁻¹, corresponding to 100 Mpc. Another hole in the distribution of recession velocities exists between 3196 and 3629 km s⁻¹. We are therefore rather confident of the completeness of our list of groups up to 3500 km s⁻¹.

We applied the same hierarchical algorithm as in Gourgoulhon et al. (1992), cutting the hierarchy at a density level of $8 \cdot 10^9 L_{\odot} \text{ Mpc}^{-3}$, and adopting a transition velocity of 250 km s^{-1} . We find 18 groups, containing 95 galaxies among the 160 with $V < 7500 \text{ km s}^{-1}$ (59 %). 18 other galaxies belong to pairs, and 19 are isolated members of associations (regions where the density level is five times less than for groups). This leaves 28 apparently isolated galaxies. In fact, two of them probably belong to the Local Group (IC 5152) and the Sculptor Group (ESO 347-8), and 13 of them have a recession velocity larger than 3500 km s^{-1} . The list of the remaining 13 isolated galaxies is given in Table 3, and the list of the 18 groups with their members and their characteristics in Table 4. The following characteristics are given: L_B is the total luminosity in the B -band in units of $10^9 L_{\odot}$. V_V^1 is the line-of-sight luminosity-weighted velocity dispersion in km s^{-1} . R_V is the virial radius in Mpc. M/L is the virial mass to blue luminosity ratio in M_{\odot}/L_{\odot} . t_{cr} is the crossing time in units of 10^9 yr .

Table 3. List of 13 isolated galaxies

PGC	Name	α_{1950}	δ_{1950}	V_{\odot}	σ	Note
68582	ESO 344-21	22 16 51.0	-40 55 12	3196	30	
68661	ESO 345-02	22 19 20.0	-40 20 30	2235	27	
69103	ESO 345-21	22 29 44.0	-38 18 24	3141	49	
69539	NGC 7361	22 39 31.0	-30 19 12	1245	5	*
69998	ESO 346-14	22 52 17.0	-38 51 06	2700	10	
70039	IC 5269A	22 53 09.2	-36 36 58	2877	10	
70427	NGC 7476	23 02 16.0	-43 22 12	2952	34	
70505	NGC 7484	23 04 19.0	-36 32 42	2732	29	
70565	ESO 469-15	23 06 13.0	-31 07 48	1631	10	
70806	ESO 347-03	23 12 08.0	-38 07 48	2812	30	
70966	ESO 407-14	23 14 57.0	-35 03 54	2755	10	
72300	NGC 7744	23 42 21.0	-43 11 18	3069	30	*
72444	NGC 7755	23 45 15.8	-30 47 51	2963	5	*

Notes:

NGC 7361: listed in Tully (1988) as isolated member of our association VI-12.

NGC 7744: listed as isolated in Tully (1988).

NGC 7755: listed as isolated in Tully (1988).

Most of the detected groups were already known. For instance, NGC 7049, NGC 7144, NGC 7196, NGC 7213 groups and association VI-12 (called Grus group) appear in Sandage (1975); NGC 7079 group is quoted by de Vaucouleurs (1975). The name of these groups in Tully's (1988) Nearby Galaxies Catalog is given for cross-reference: our study encompasses parts of regions 19 and 61 of this catalog. The name of an association is composed of the region number (roman Fig. I or VI) and the association number, as described in Fouqué et al. (1992). Two new associations are evidenced below 3500 km s^{-1} . Only one association is detected between 3500 and 7500 km s^{-1} , which contains four groups.

For each group, we give in Table 4 its total luminosity in B -band, corrected for incompleteness (see Gourgoulhon et al. 1992, for details). The large luminosities of distant groups may be partly due to this correction. Below 3500 km s^{-1} , the most significant groups in terms of luminosity are NGC 7582, IC 1459, NGC 7079 and NGC 7213. The median line-of-sight luminosity-weighted velocity dispersion is 90 km s^{-1} , part of which is due to the measurement uncertainty. The median virial radius is 0.53 Mpc . The median mass-to-blue luminosity ratio is $75 M_{\odot}/L_{\odot}$. The median crossing time is $2.0 \cdot 10^9 \text{ yr}$, showing that our aggregates are gravitationally bound entities and not spurious concentrations (the only suspect case is the NGC 7713 group). Now, the time to reach a virialized state is about 1.5 collapse time (Gott & Rees 1975). For a virialized group, the collapse time over crossing time ratio is 2π . We thus expect a mean virialization time slightly larger than the Hubble time. Indeed, only one group (ESO 342-27) has a short enough collapse time ($3.6 \cdot 10^9 \text{ yr}$) to be virialized. The correction for incompleteness involved into the calculation of the total luminosity of this group is $\beta = 2.35$. If we neglect this factor, assuming that no fainter galaxy belongs to the group, its collapse time increases as $\beta^{1/2}$, and amounts to $5.5 \cdot 10^9 \text{ yr}$. It seems therefore that its virialized status cannot be contested because of its large distance.

Figure 3 shows the projected distribution of the galaxies in our sample. Groups members are identified by special symbols.

Figure 4 shows an iso-number density plot of the 122 galaxies with recession velocities smaller than 3500 km s^{-1} . The density value assigned to each galaxy is calculated as 11 divided by the area covered by the 10 galaxies closest to it. The four most luminous groups are evidenced.

5. Discussion

Our main goal, when we embarked upon this survey, was to understand the large dispersion observed in the M/L ratios of the groups in our all-sky survey, and to determine if certain parameters can help to understand this dispersion. Our present deeper survey has not reduced the dispersion, with M/L values varying between 9 and $442 M_{\odot}/L_{\odot}$. If we now restrict the discussion to groups with at least 5 galaxies, to reduce effects of projection factors and poor statistics, we get 6 groups, which we will compare in more detail.

The uncertainty of our M/L estimate depends upon both mass and luminosity errors. As our estimate of L involves correcting factors for incompleteness, it is difficult to estimate an error bar. We therefore concentrate our effort on mass determination, in three directions: we first correct the dispersion velocity for measurement uncertainties, and estimate a 1σ confidence interval of the unweighted line-of-sight dispersion velocity, using the pre-

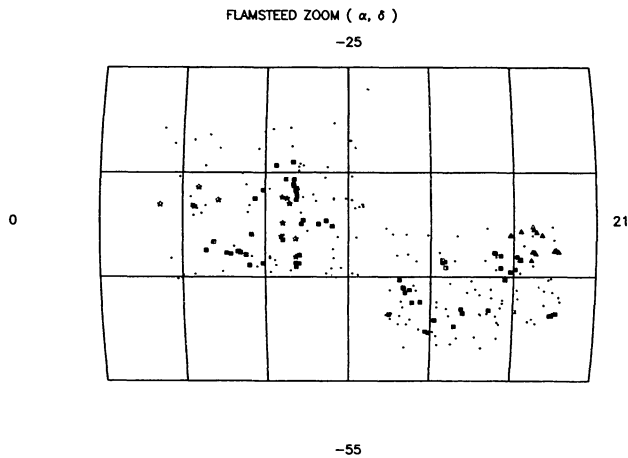


Fig. 3. Projected distribution of the 278 galaxies, in a sinusoidal (Flamsteed) projection. Filled symbols represent members of the 18 groups (stars if $V < 1500 \text{ km s}^{-1}$, squares if $1500 < V < 3500 \text{ km s}^{-1}$, and triangles if $3500 < V < 7500 \text{ km s}^{-1}$). Dots represent galaxies not assigned to groups, or galaxies with $V > 7500 \text{ km s}^{-1}$.

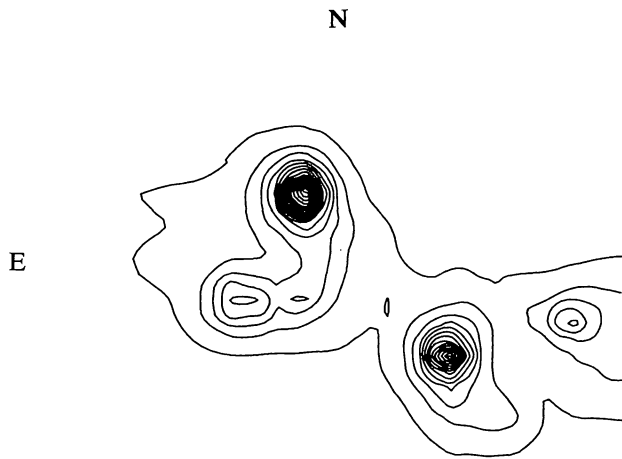


Fig. 4. Iso-number density plot of galaxies with recession velocities smaller than 3500 km s^{-1} . North is up and east at left. The densest concentration is the IC 1459 group, followed by the NGC 7213 one. The left-most concentration is the NGC 7582 group, and the right-most one corresponds to the NGC 7079 group. The lowest contour corresponds to 1 galaxy per Mpc^2 , and an interval corresponds to 1 galaxy per Mpc^2 . The peak is at 18 galaxies per Mpc^2 .

cepts of Danese et al. (1980). The result is given in Col. 3 of Table 5, and used to estimate a minimal range of M/L values, given in Col. 4 of Table 5.

Then, we make the following simulation: we keep fixed the positions on the sky of the galaxies in a group, but we mix their velocities and their luminosities. As there are many possible combinations ($N!^2$), we choose at random 1000 possibilities, and compute a new M/L ratio. We then compare it to the observed M/L , and compute the ratio of both numbers. The mean value of the 1000 trials and their rms dispersion are given in Col. 5 and 6 of Table 5. An average value significantly different from one implies that the observed configuration is rather particular. This is the case of the NGC 7582 group, which has the lowest observed M/L ratio. On the other hand, the highest M/L ratio, observed in the NGC 7424 group, is confirmed by our simulation. In fact, the mean ratio $M_{\text{sim}}/M_{\text{obs}}$ is a measure of the ratio unweighted over weighted estimators of the virial mass.

Finally, we compute the Heisler et al. (1985) estimators of mass, and compare them to the virial mass. The projected mass is computed assuming isotropic orbits and equal masses. The ratios of projected mass, average mass and median mass over unweighted virial mass are given in Col. 7, 8 and 9 of Table 5.

In order to see if M/L varies systematically with some characteristics of the groups, we wish to introduce two characteristic numbers: the first one, $N1$, is the ratio of the luminosity of the most luminous galaxy to the total luminosity of the group (corrected for incompleteness). It measures the dominance of the group by one member: the hypothesis of equal masses for all members corresponds to $N1$ between 0.08 and 0.13 for our 6 groups. The second number, $N2$, is a kind of measure of the stability of the group in our hierarchical algorithm, and has to do with the virialization state of the group. It depends upon the number of subcondensations in a group. Such a subcondensation is defined by a density level five times higher than the group. $N2$ is the difference between the number of galaxies in the most populated subcondensation and the number of subcondensations, divided by the total number of galaxies in the group. Let us take two extreme examples to understand the concept: first, imagine a stable group with N members, all within the same subcondensation: therefore, $N2 = (N - 1)/N$, which approaches one when N increases. On the contrary, imagine a sparse group with each member in its own subcondensation; therefore, $N2 = (1 - N)/N$, approaching -1 when N increases. Briefly, a compact stable and virialized group will have $N2 \lesssim 1$, while a dispersed one will have $N2 \gtrsim -1$. $N1$ and $N2$ are given in Col 10 and 11 of Table 5.

6. Conclusions

Several conclusions can be drawn from the results of Table 5, being aware that our statistical basis is very reduced.

The low observed M/L ratio of the NGC 7582 group appears to be due to a particular configuration of the

Table 4. List of 18 groups, their characteristics, and their members

Ass.	Group	α_{1950}	δ_{1950}	V_{\odot}	L_B	V_V^1	R_V	M/L	t_{cr}	Members
New	ESO 342-27	21 13.6	-42 30	5228	319	140	0.11	10	0.6	E286-82 E287-2 E342-26 E342-27
	IC 5105	21 21.6	-40 37	5237	369	189	0.93	125	1.2	I5105 I5105A E342-36 E342-45
	NGC 7060	21 23.3	-42 55	5006	246	160	0.64	93	2.6	N7057 N7060 N7072 N7072A E287-16 E287-26
	NGC 7087	21 30.1	-40 56	5037	129	91	0.24	21	3.6	N7087 E343-1 E343-7 E287-7 E287-32
	Others									N7041 N7049 E235-85
New	NGC 7049 (T61-10)	21 14.7	-48 42	2098	69	138	0.30	117	0.5	
VI-16	NGC 7079 (T61-6)	21 31.4	-43 37	2527	112	111	0.98	149	3.6	N7070 N7070A N7079 N7097 N7097A E287-37 E287-39 E287-41 E287-43 N7107 I5105B E236-6 E287-9 E287-13
	Others									N7144 N7145 N7155 E236-35
VI-14	NGC 7144 (T61-12)	21 49.3	-48 32	1921	56	58	0.54	45	4.1	N7213 N7232 N7232B? N7233 I5170 I5181 E238-4 E289-5 E289-11 N7151
	NGC 7213 (T61-11)	22 08.9	-46 53	1816	87	111	0.42	83	2.2	N7162 N7162A N7166 E288-25 N7232A I5171
	Other									N7196 N7200 E237-31
VI-17	NGC 7166 (T61-9)	21 56.8	-43 42	2376	61	89	0.28	51	1.2	E237-19 E237-52
	Others									N7368 E345-46 E346-1
New	NGC 7196 (T61-7)	22 02.8	-50 16	2904	53	37	0.52	19	3.7	
	Others									N7307
VI-15	NGC 7368 (T61+14)	22 42.7	-39 47	2313	45	90	0.71	180	1.6	N7404 N7410 E346-25 N7412 I5267 I5267A I5267B
	Other									N7418A I5264 I5269
VI-12	NGC 7410	22 52.3	-39 56	1763	53	49	1.20	77	1.8	N7418 N7421 I1459 I5269B I5269C I5270 I5271 E406-31 E407-2 E407-7 E407-9
	IC 5267	22 53.7	-43 25	1691	58	61	0.41	36	1.9	N7496 N7531 N7552 N7582 N7590 N7599 N7632 I5325 E291-24 E347-2 E347-20 N7545 I5240 E289-42 E292-14 E345-42 E347-29
	IC 5264 (T61-15)	22 54.3	-36 43	2104	28	70	0.30	74	1.4	N7412A N7424 N7456 N7462 I5273 E406-40 E406-42
	IC 1459 (T61-17)	22 55.8	-36 24	1673	139	127	0.60	97	2.8	N7713 I5332 E347-17 E348-9
	NGC 7582 (T61-16)	23 15.3	-42 46	1591	178	60	0.32	9	4.6	
	Others									
I-36	NGC 7424 (T19-6)	22 57.2	-40 34	1076	44	138	0.74	442	1.7	
I-37	NGC 7713 (T19-7)	23 32.2	-37 14	698	13	9	0.66	5	12.8	

Table 5. M/L ratio for the 6 most populated groups (see text)

Group name	N	σ_V	$\left(\frac{M_V}{L}\right)_{obs}$	$\left\langle \frac{M_{aim}}{M_{obs}} \right\rangle$	σ	M_P/M_V^{uw}	M_A/M_V^{uw}	M_M/M_V^{uw}	$N1$	$N2$
NGC 7582	11	121^{+40}_{-21}	5-15	6.84	3.42	2.29	1.60	0.89	0.18	0.55
NGC 7213	9	144^{+61}_{-36}	35-158	1.69	1.07	3.05	2.56	2.09	0.41	0.33
NGC 7060	6	157^{+90}_{-38}	37-205	0.90	0.26	1.80	1.26	1.40	0.12	0.
IC 1459	11	120^{+40}_{-22}	53-167	1.18	0.44	1.63	0.83	1.07	0.27	0.18
NGC 7079	9	98^{+42}_{-26}	58-284	0.82	0.26	1.42	1.14	1.35	0.19	-0.22
NGC 7424	7	175^{+84}_{-34}	214-892	1.31	0.55	1.64	1.45	1.70	0.27	0.

galaxies. The unweighted virial mass to luminosity ratio is well within the range of other groups.

The high values of the ratios M_P/M_V^{uw} , M_A/M_V^{uw} and M_M/M_V^{uw} of the NGC 7213 group are probably due to the violation of one underlying hypothesis made to compute these masses, namely that the galaxies in the group have equal masses. The high $N1$ value for this group contradicts this hypothesis. Remember that for a group dominated by a massive central member, the projected mass estimator is divided by two (Bahcall & Tremaine 1981).

The ratio M_P/M_V^{uw} appears to be larger than the two other ratios, M_A/M_V^{uw} and M_M/M_V^{uw} : the mean value for projected masses is about 2, while it is about 1.5 for average and median masses. This possibly corresponds to an intermediate situation between equal masses and dominant central galaxy (see previous point). An average coefficient between these two extreme cases would give M_P values lower by a multiplicative factor 0.75, and this would put the three ratios at the same level. However, this common level still corresponds to masses 50 % higher than the unweighted virial mass. No correlation appears between $N1$ or $N2$ on one hand, and the M/L ratio on the other hand. Further analysis in progress of other groups will confirm or deny this first impression. The aim of this first paper was to define the concepts.

Acknowledgements. P.F. wishes to thank Georges Paturel for stimulating discussions concerning group algorithms in the early phase of this project. Leopoldo Infante and Hector Cuevas help us producing the sinusoidal projection. D.P. acknowledges the Grupo de Astrofísica of the Universidad Católica de Chile for its hospitality. This research has been partially funded by FONDECYT Grants 90/371 and 92/754, and supported by the bilateral cooperation program in Astrophysics between CONICYT and the Cooperation Service of France.

References

- Bahcall J.N., Tremaine S. 1981, *ApJ* 244, 805
 Bottinelli L., Durand N., Fouqué P., Garnier R., Gouguenheim L., Paturel G., Petit C., Teerikorpi P. 1992, *A&AS*, in press
 Chincarini G., Tarengi M., Sol H., Crane P., Manousouyanaki I., Materne J. 1984, *A&AS* 57, 1
 da Costa L.N., Pellegrini P.S., Davis M., Meiksin A., Sargent W.L.W., Tonry J.L. 1991, *ApJS* 75, 935
 Danese L., de Zotti G., di Tullio G. 1980, *A&A* 82, 322
 de Vaucouleurs G. 1975, in: *Stars and Stellar Systems*, Vol. 9, *Galaxies and the Universe*, eds. A. Sandage, M. Sandage and J. Kristian, University of Chicago Press, Chicago, p.557
 de Vaucouleurs G., de Vaucouleurs A., Corwin H.G., Buta R.J., Paturel G., Fouqué P. 1991, *Third Reference Catalogue of Bright Galaxies*, ed. Springer-Verlag (RC3)
 Dressler A., Shectman S.A. 1988, *AJ* 95, 985
 Fairall A.P. 1980, *MNRAS* 192, 389
 Fouqué P., Gourgoulhon E., Chamaraux P., Paturel G. 1992, *A&AS* 93, 211
 Gott J.R., Rees M.J. 1975, *A&A* 45, 365
 Gourgoulhon E., Chamaraux P., Fouqué P. 1992, *A&A* 255, 69
 Heisler J., Tremaine S., Bahcall J.N. 1985, *ApJ* 298, 8
 Karachentseva V.E. 1973, *Soob. Special Astrophys. Obs.*, 8
 Lauberts A., Valentijn E.A. 1989, *The Surface Photometry Catalogue of the ESO-Uppsala Galaxies*, European Southern Observatory (ESOLV)
 Materne J. 1978, *A&A* 63, 401
 Maurice E., Mayor M., Andersen J., Ardeberg A., Benz W., Lindgren H., Imbert M., Martin N., Nordström B., Prévot L. 1984, *A&AS* 57, 275
 Paturel G., Bottinelli L., Fouqué P., Fruscione A., Gouguenheim L. 1987, *Bull. Inform. CDS*, 33, 9
 Paturel G., Fouqué P., Bottinelli L., Gouguenheim L. 1989a, *A&AS* 80, 299
 Paturel G., Fouqué P., Bottinelli L., Gouguenheim L. 1989b, *Monographies de la Base de Données Extragalactiques*, N° 1 (Vols. I, II, III) (PGC)
 Paturel G., Petit C., Kogoshvili N., Dubois P., Bottinelli L., Fouqué P., Garnier R., Gouguenheim L. 1991, *A&AS* 91, 371
 Proust D., Quintana H., Mazure A., da Souza R., Escalera E., Sodré Jr. L., Capelato H.V. 1992, *A&A* 258, 243
 Sandage A. 1975, *ApJ* 202, 563
 Tonry J., Davis M. 1979, *AJ* 84, 1511
 Tully R.B. 1987, *ApJ* 321, 280
 Tully R.B. 1988, *Nearby Galaxies Catalog*, ed. Cambridge University Press